Supporting Information

Table of Contents

Experimental section	3
Materials and methods	3
Calculations	4
Synthesis of **1**.	4
Fig. S1. ^{1}H NMR spectrum of compound **1** in $CDCl_3$ at 27 °C.	6
Fig. S2. ^{13}C NMR spectrum of compound **1** in $CDCl_3$ at 27 °C.	6
Fig. S3. Neat FT-IR spectrum of compound **1**.	7
Fig. S4. TGA curve of 1 from 30 to 900 ^{o}C under a nitrogen atmosphere with a heating rate of $^{o}C\ min^{-1}$.	7
Fig. S5. The solution state UV-vis spectra of **L**.HI and **1** in DCM (C = $4x10^{-4}$ M) at RT.	8
Fig. S6. The solid state (Excitation at 290 nm) and solution state (in DCM; Excitation at 375 nm; C = 4×10^{-5} M) fluorescence spectra of **L**.HI and **1** at RT.	8
Fig. S7. (I) The solution state (Excitation at 375 nm) at RT in CH_2Cl_2 (C = 4×10^{-5} M) and solid-state emission spectra of **1** (Excitation at 290 nm) at RT using crystals. (II) Commission Internationale de L'Eclairage (CIE) 1931 coordinates of **1** in solid state.(III) crystalline sample of **1** (a) under normal light and (b) under UV light with 365 nm.	9
Fig. S8. Commission Internationale de L'Eclairage (CIE) 1931 coordinates of **1** in solid state and solution state.	10
Fig. S9. Solution state (in DCM; Excitation at 375 nm; C = 4×10^{-5} M) emission spectra (before degas and after degas with argon) of **1** at RT.	10
Fig. S10. Solution state (in DCM; Excitation at 375 nm; C = 4×10^{-6} M) emission spectra (before degas and after degas with argon) of **1** at RT.	11
Fig. S11. Solution state (in DCM; Excitation at 375 nm; C = 4×10^{-7} M) emission spectra (before degas and after degas with argon) of **1** at RT.	11
Fig. S12. Photoluminescence decay profiles of **1** in DCM ($1x10^{-5}$ M). (IRF = Instrument Response Function).	11
Fig. S13. Photoluminescence decay profiles of **1** in DCM ($1x10^{-6}$ M). (IRF = Instrument Response Function).	12
Fig. S14. Photoluminescence decay profiles of **1** in DCM ($1x10^{-7}$ M). (IRF = Instrument Response Function).	12
Fig. S15. Photoluminescence decay profiles of crystal **1**. (IRF = Instrument Response Function).	12
Fig. S16. The presence of a weak aurophillic interaction in **1**.	13
Fig. S17. Crystal packing of complex **1** shows intermolecular C- Cl···H interactions and C(sp^2) -H···π interactions.	13
Fig. S18. The calculated UV-vis spectrum of **1**.	14
Fig. S19. The orbitals involved in the transition of **1**.	15
Table S1. Solid-state structural parameters of **1**.	16

Table S2. Fitting parameters of fluorescence decay of **1** in solution state ($1x10^{-5}$ M). (RAx = Relative amplitude of x^{th} component).	17
Table S3. Fitting parameters of fluorescence decay of **1** in solution state ($1x10^{-6}$ M). (RAx = Relative amplitude of x^{th} component).	17
Table S4. Fitting parameters of fluorescence decay of **1** in solution state ($1x10^{-6}$ M). (RAx = Relative amplitude of x^{th} component).	17
Table S5. Fitting parameters of fluorescence decay of **1** (Crystal). (RAx = Relative amplitude of x^{th} component).	17
Tale S6. Excitation energies and oscillator strengths of **1**.	18
Table S7. AIM Analysis (all in atomic units, a. u.)	20
Table S8. NBO Analysis	20
Table S9. DFT Cartesian coordinates of **1**.	21
References	22

Experimental section

Materials and methods

The reactions were carried under inert gas atmosphere using standard Schlenk line techniques. The starting materials were purchased from the commercial sources and used. The 1-methyl-5-phenyl-3-(2-diphenyl methyl-4,6-dimethyl phenyl)- 1,2,3-triazolium iodide (**L**.HI) was prepared according to the previous literature methods.[1] FT-IR measurements (neat) were performed on a Bruker Alpha-P Fourier transform spectrometer. Elemental analysis was done by using a Euro EA - CHNSO Elemental Analyzer. Thermogravimetric analysis (TGA) was done by using a TASDT Q600, Tzero-press. ^{1}H and ^{13}C NMR spectra were measured by using Bruker Ultrashield-400 spectrometers at 25 °C. Chemical shifts are given relative to TMS and were referenced to the solvent resonances as internal standards, and the chemical shifts are reported in ppm and the coupling constants in Hz. UV-vis absorption spectra were recorded using a V-500 spectrophotometer (JASCO, Tokyo, Japan). Steady-state photoluminescence spectra were obtained using a F-7000 fluorescence spectrophotometer (Hitachi, Tokyo, Japan). Photoluminescence quantum yields were measured using a calibrated integrating sphere system (Hitachi). Photoluminescence decay of **1** was measured using Hamamatsu TDC Unit M12977 from the wavelength range of luminescence 485 nm. The measurement was carried out using a laser pulse at 340 nm (FWHM; 5 MHz). The suitable single crystals of **1** for the single-crystal X-ray analysis were obtained from their reaction mixture in dichloromethane and hexane (1:1) at room temperature. The suitable single crystals for X-ray structural analysis were mounted at room temperature (298 K) in inert oil under an argon atmosphere. The crystal structure of **1** was measured on an Oxford Xcalibur 2 diffractometer. Using Olex2, the structure was solved with the ShelXS structure solution program using Direct Methods and refined with the olex2.refine refinement package using Gauss-Newton minimization.[2] Absorption corrections were performed on the basis of multi-scans. Non-hydrogen atoms were anisotropically refined. CCDC 2104801 (**1**) contains the supplementary crystallographic data for this paper. These data can be obtained free of charge from the Cambridge Crystallographic Data Centre via www.ccdc.cam.ac.uk/data_request/cif or from the Cambridge Crystallographic Data Centre, 12 Union Road, Cambridge CB2 1EZ, UK; fax: +44 1223 336 033; or e-mail: deposit@ccdc.cam.ac.uk.

Calculations

All the calculations were done using the Gaussian 16 suite of program.[3] The input files were generated using GaussView, Version 6.[4] The structural parameters of the **1** complex was adopted from X-ray crystal structure data. Density Functional Theory (DFT) and Time-dependent density-functional theory (TD-DFT) calculations were carried out at the B3LYP level of theory using def2-TZVP valence basis set for gold and 6-31G basis set for chlorine, carbon, hydrogen and nitrogen. For gold, the Stuttgart-Dresden effective core potential (REF), denoted as the def2 or SDD in Gaussian was used to describe 60 core electrons (ncore = 60).[5] Vibrational frequency calculations were carried out to ensure the structure is minima on the potential energy surface. The atoms-in-molecule (AIM) analysis was performed Using the AIMALL software package,[6] with B3LYP/def2-TZVP wave functions to find topological features of the electron density. AIM analysis is established on Bader's theory.[7]

Synthesis of 1

To a mixture of **L**.HI (100 mg, 0.19 mmol) in dry DCM (5 mL), silver oxide (114 mg, 0.49 mmol) was added in the absence of light and stirred for 5 h at room temperature. Then Au(tht)Cl (63 mg, 0.19 mmol) was added and stirred for overnight at room temperature. The reaction mixture was filtered on a pad of Celite, the solvent was evaporated under vacuum and the crude product was purified by column chromatography (*n*-hexane: DCM, 1:1). Evaporation of the solvent gave the analytically pure product **1** as a white solid. Yield: 75% (Based on **L**.HI). Mp: 284-287 °C. Elemental analysis for $C_{30}H_{27}IN_3AuCl$ (MW: 557.47) (%): Calcd. C, 54.43; H, 4.11; N, 6.35. Found C, 54.3 H, 4.1; N, 5.2. ^{1}H NMR (400.130 MHz, $CDCl_3$): δ 7.66 (ddd, 2H, Ar-*H, J* = 5.5 Hz, *J* = 2.9 Hz, *J* = 1.5 Hz), 7.51–7.57 (m, 3H, Ar-*H*), 7.28 (d, 2H, Ar-*H, J* = 7.5 Hz), 7.14–7.24 (m, 6H, Ar-*H*), 7.06 (d, 1H, Ar-*H, J* = 0.5 Hz), 6.87–6.93 (m, 2H, Ar-*H*), 6.59 (s, 1H, Ar-*H*), 5.88 (s, 1H, C*H*Ph_2), 3.73 (s, 3H, N-CH_3), 2.29 (s, 3H, CH_3), 2.03 (s, 3H, N-CH_3). ^{13}C NMR (101.612 MHz, $CDCl_3$): δ 160.33 (*C*-Au), 146.49(C_{trz}), 142.13(C_{Ar}), 141.11(C_{Ar}), 140.73(C_{Ar}), 140.69(C_{Ar}), 135.18(C_{Ar}), 134.59(C_{Ar}), 130.39(C_{Ar}), 130.28(C_{Ar}), 129.71(C_{Ar}), 129.49(C_{Ar}), 129.26(C_{Ar}), 129.20(C_{Ar}), 129.11(C_{Ar}), 128.58(C_{Ar}), 128.12(C_{Ar}), 126.77(C_{Ar}), 126.34(C_{Ar}), 126.10 (C_{Ar}),

52.24 (*C*HPh$_2$), 37.48 (N-*C*H$_3$), 21.569 (*C*H$_3$), 17.57 (*C*H$_3$). FT-IR (cm^{-1}, neat): 3031(m), 2924(m), 2311(b), 2156(b), 2061(b), 1889(m), 1742(b), 1599(s), 1542(m), 1475(m), 1380(m), 1324(b), 1287(m), 1192(s), 1076(s), 1024(s), 918(m), 859(s), 7749(s), 761(s), 627(m), 551(m).

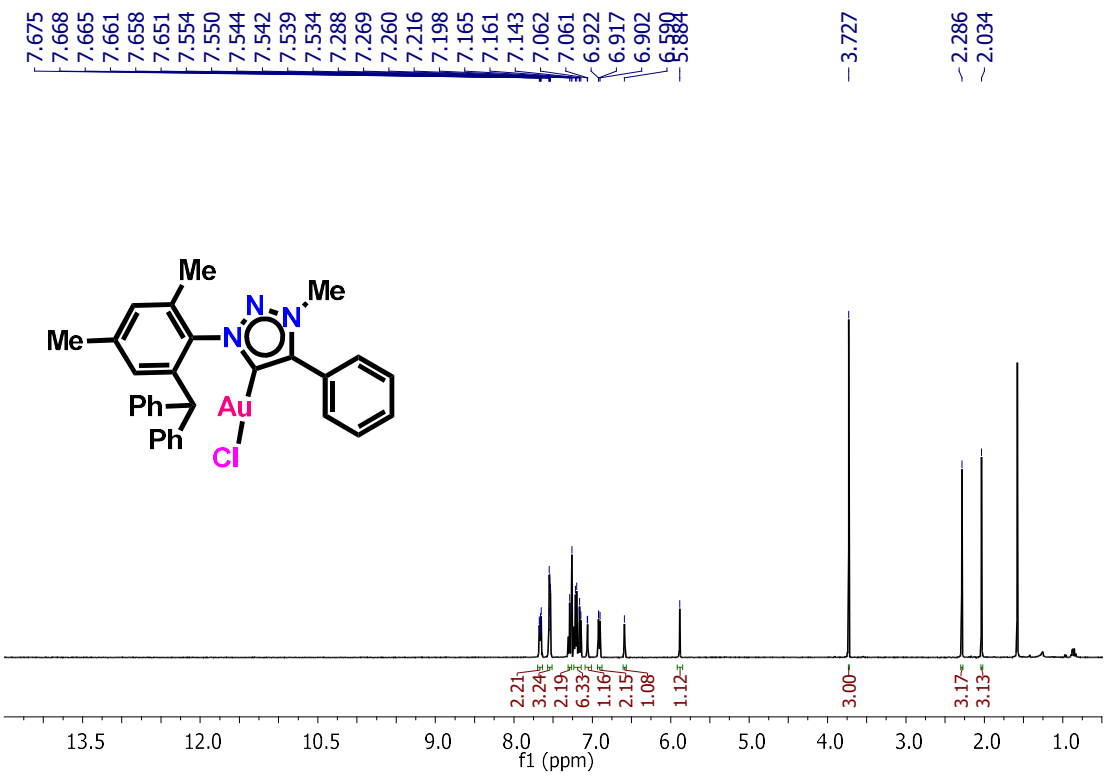

Fig. S1. ^{1}H NMR spectrum of compound **1** in $CDCl_3$ at 27 °C.

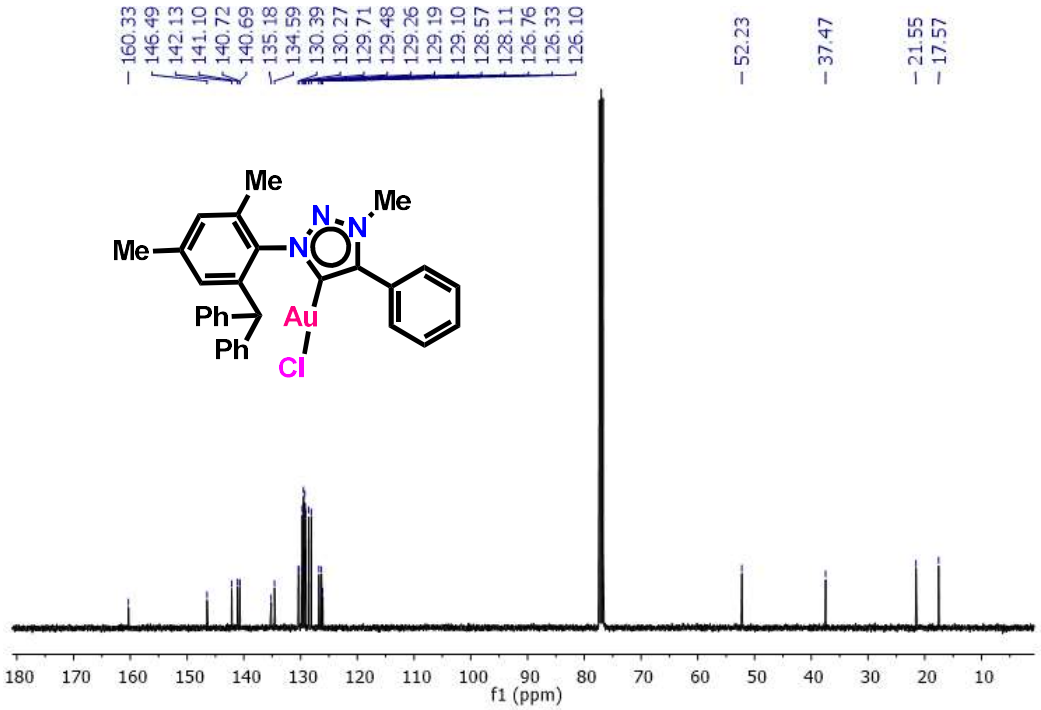

Fig. S2. ^{13}C NMR spectrum of compound **1** in $CDCl_3$ at 27 °C.

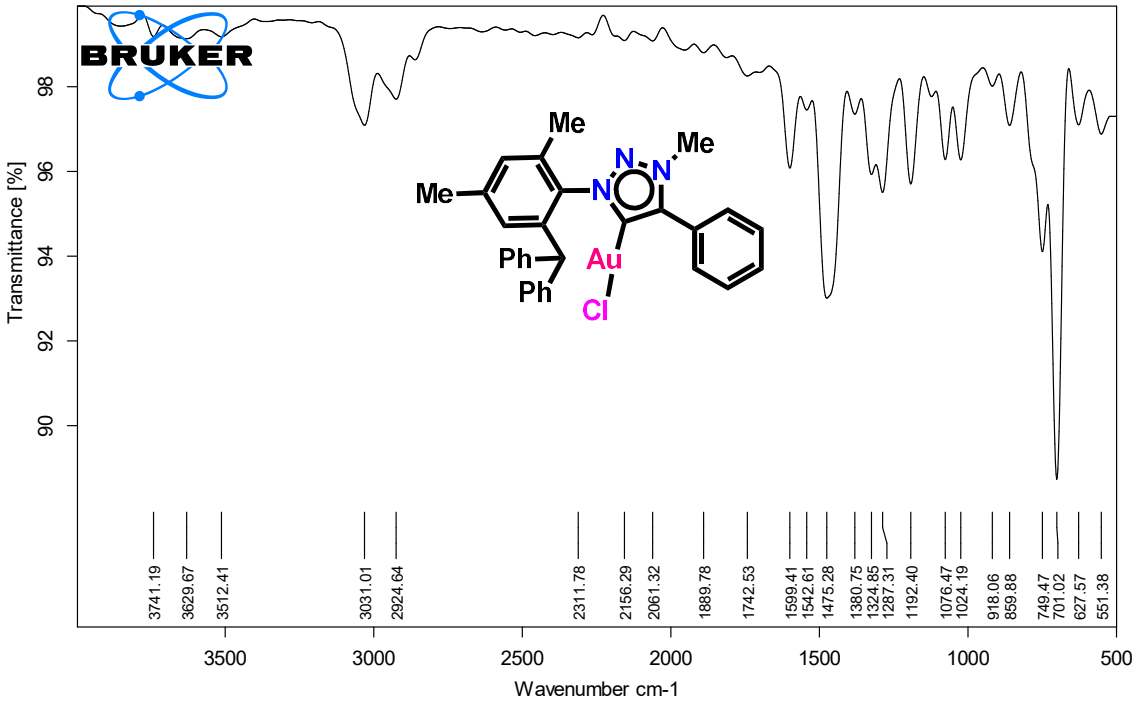

Fig. S3. Neat FT-IR Spectrum of compound **1**.

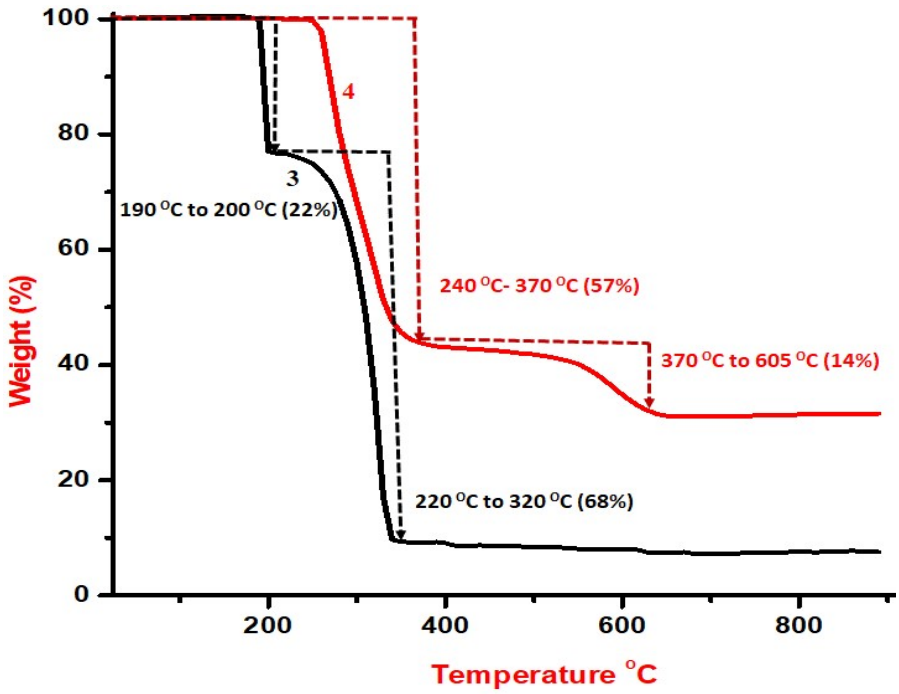

Fig. S4. TGA curve of **L**.HI and **1** from 30 to 900 °C under a nitrogen atmosphere with a heating rate of °C min^{-1}.

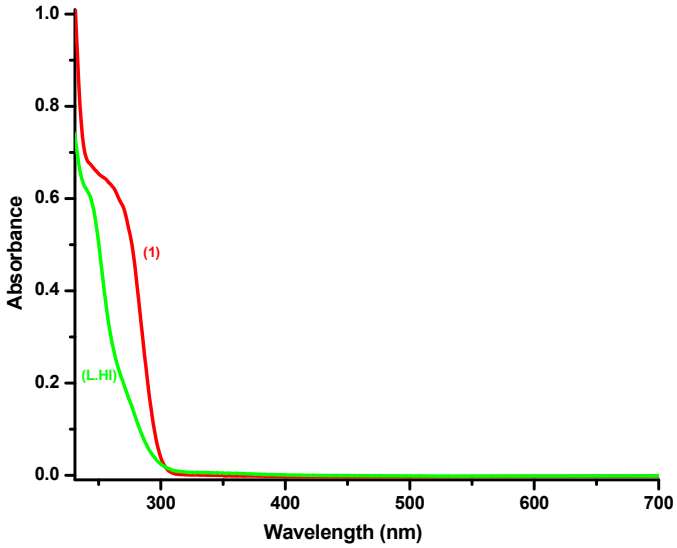

Fig. S5. The solution state UV-vis spectrum of **L**.HI and **1** in DCM (C = 4 x 10^{-4} M) at RT.

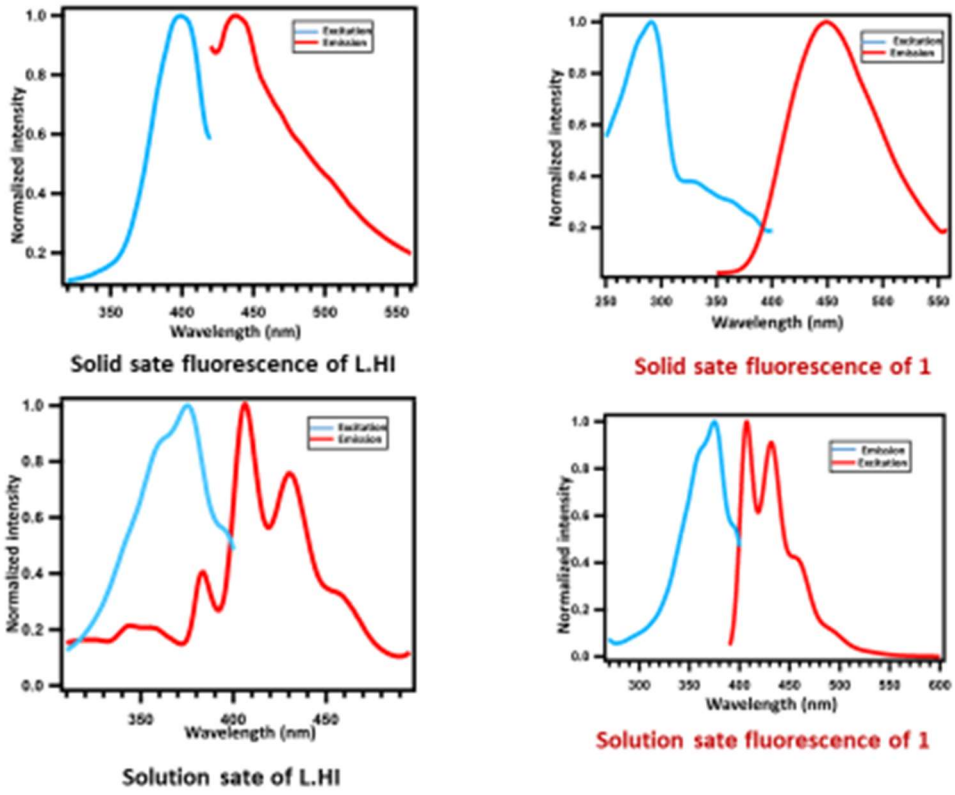

Fig. S6. The solid state (Excitation at 290 nm) and solution state (in DCM; Excitation at 375 nm; C = 4 x 10^{-5} M) fluorescence spectra of **L**.HI and **1** at RT.

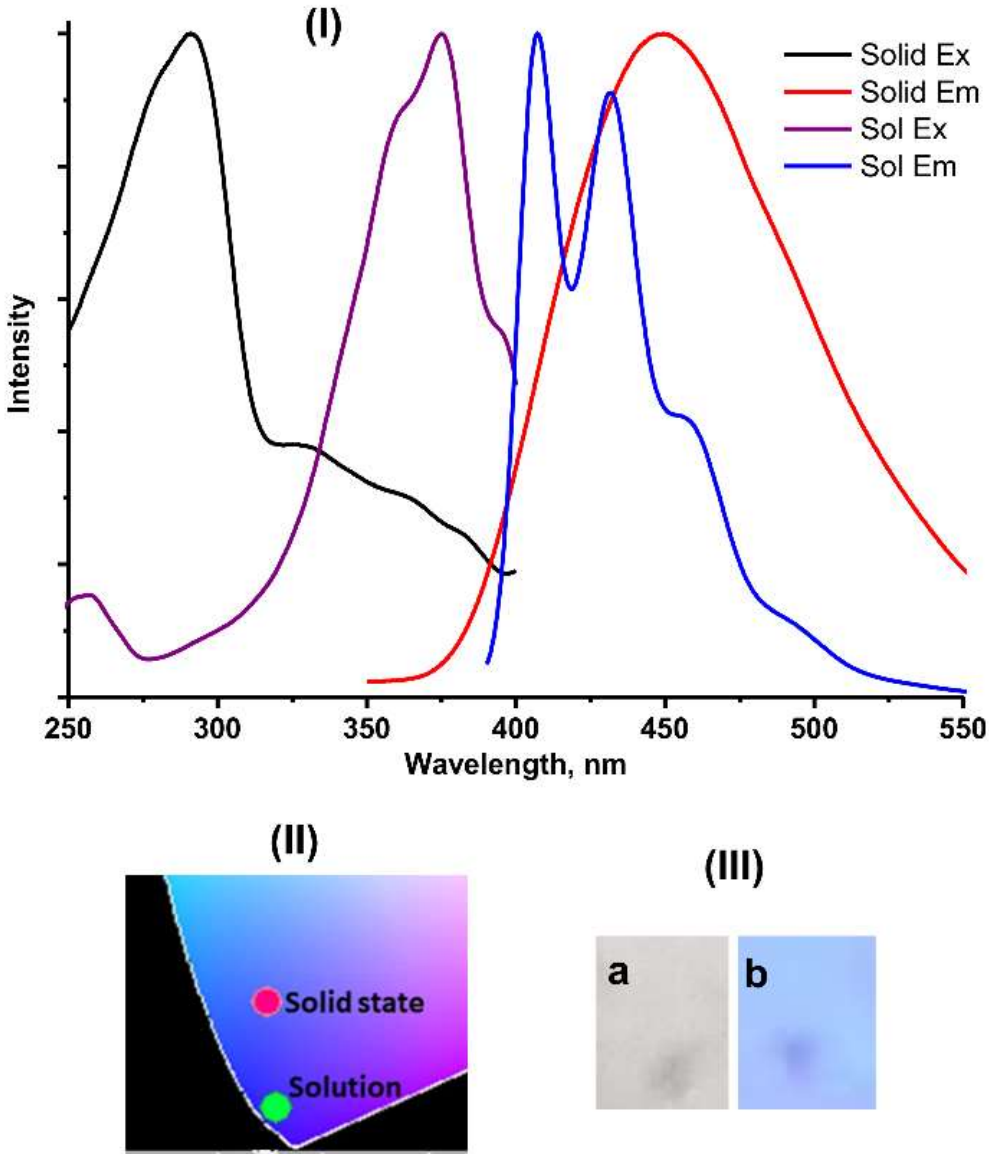

Fig. S7. (I) The solution state (Excitation at 375 nm) at RT in CH_2Cl_2 (C = 4 x 10^{-5} M) and solid-state emission spectra of **1** (Excitation at 290 nm) at RT using crystals. (II) Commission Internationale de L'Eclairage (CIE) 1931 coordinates of **1** in solid state. (III) crystalline sample of **1** (a) under normal light and (b) under UV light with 365 nm.

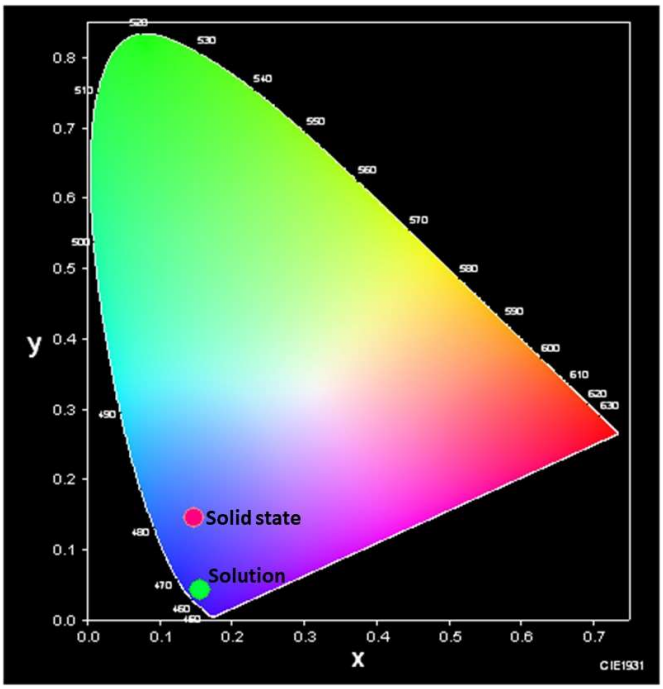

Fig. S8. Commission Internationale de L'Eclairage (CIE) 1931 coordinates of **1** in solid state and solution state.

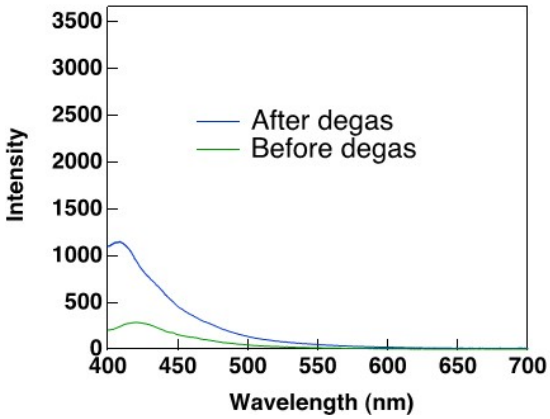

Fig. S9. Solution state (in DCM; Excitation at 375 nm; C = 4 x 10^{-5} M) emission spectra (before degas and after degas with argon) of **1** at RT.

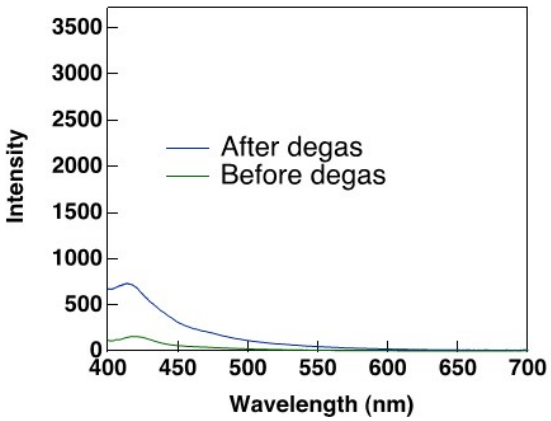

Fig. S10. Solution state (in DCM; Excitation at 375 nm; C = 4 x 10^{-6} M) emission spectra (before degas and after degas with argon) of **1** at RT.

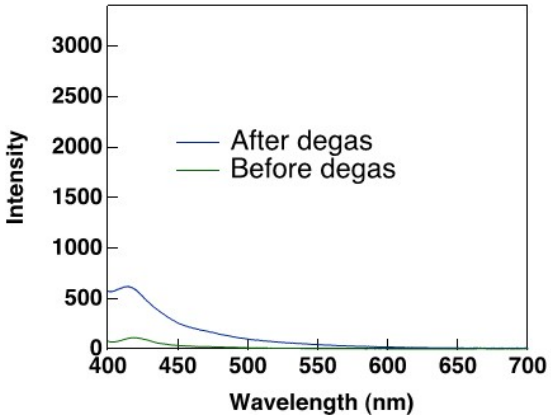

Fig. S11. Solution state (in DCM; Excitation at 375 nm; C = 4 x 10^{-7} M) emission spectra (before degas and after degas with argon) of **1** at RT.

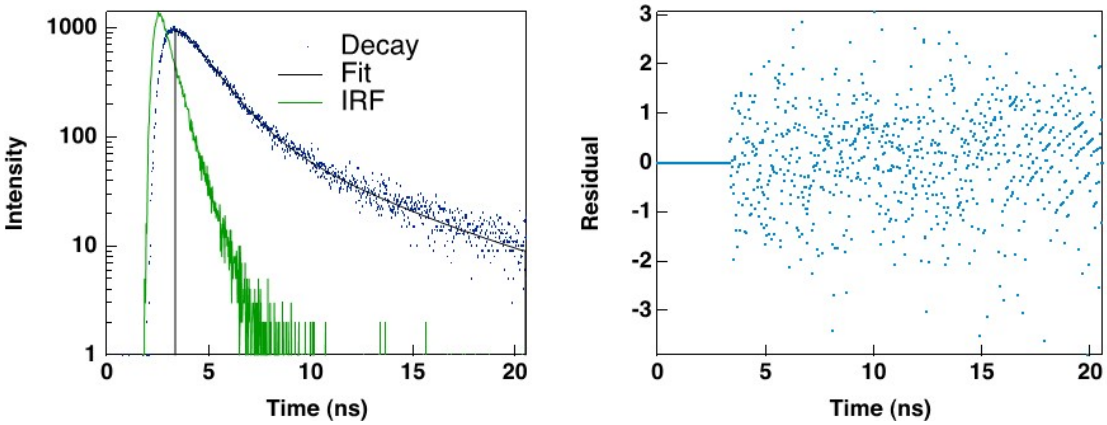

Fig. S12. Photoluminescence decay profiles of **1** in DCM (1x10^{-5}M). (IRF = Instrument Response Function).

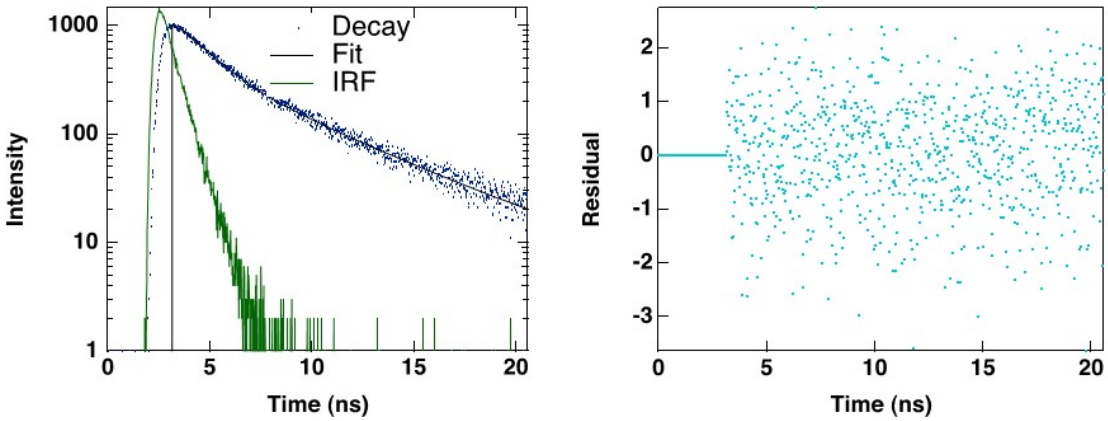

Fig. S13. Photoluminescence decay profiles of **1** in DCM ($1x10^{-6}$M). (IRF = Instrument Response Function).

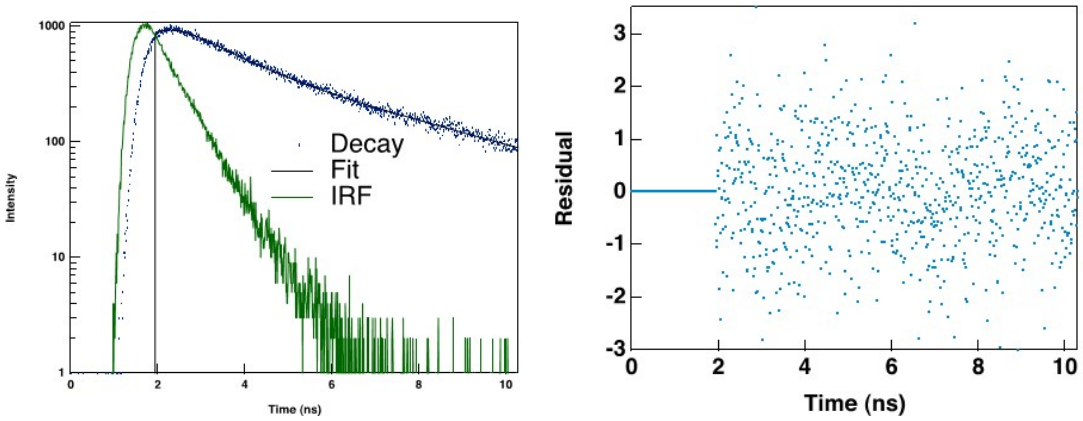

Fig. S14. Photoluminescence decay profiles of **1** in DCM solution ($1x10^{-7}$M). (IRF = Instrument Response Function).

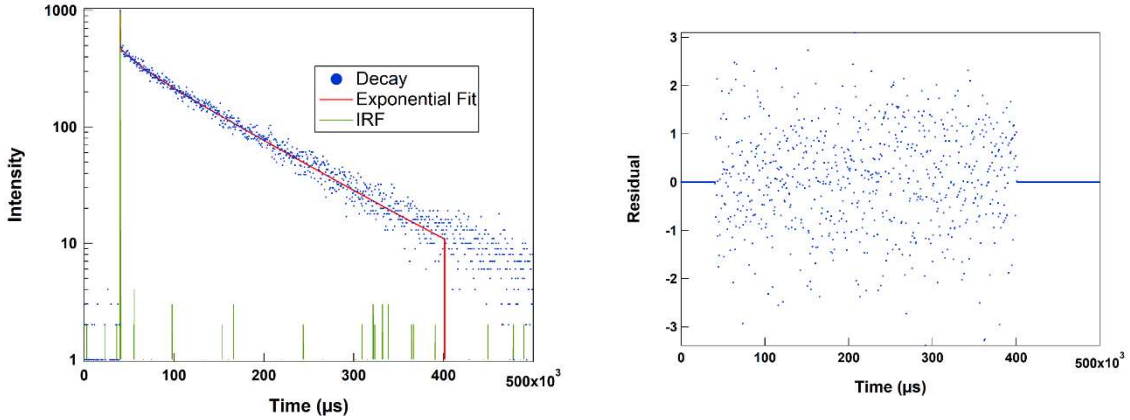

Fig. S15. Photoluminescence decay profiles of crystal **1**. (IRF = Instrument Response Function).

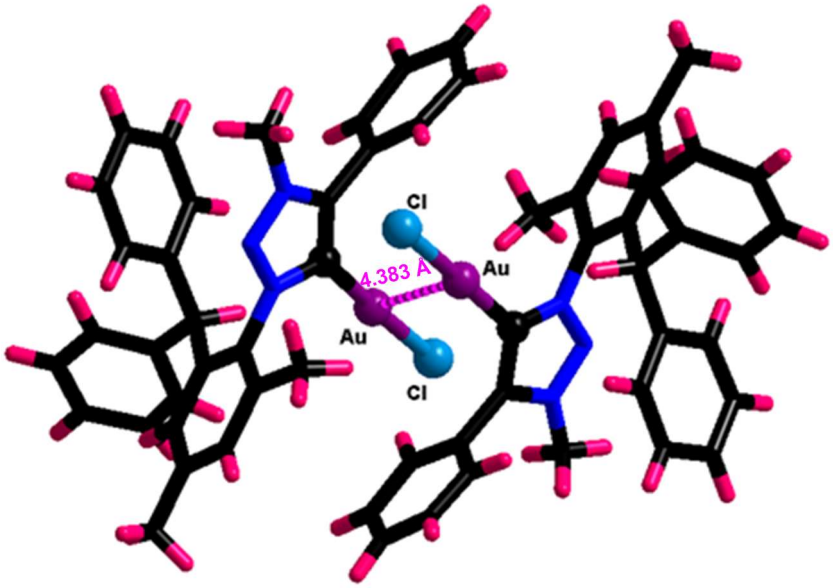

Fig. S16. The presence of a weak aurophillic interaction in **1**.

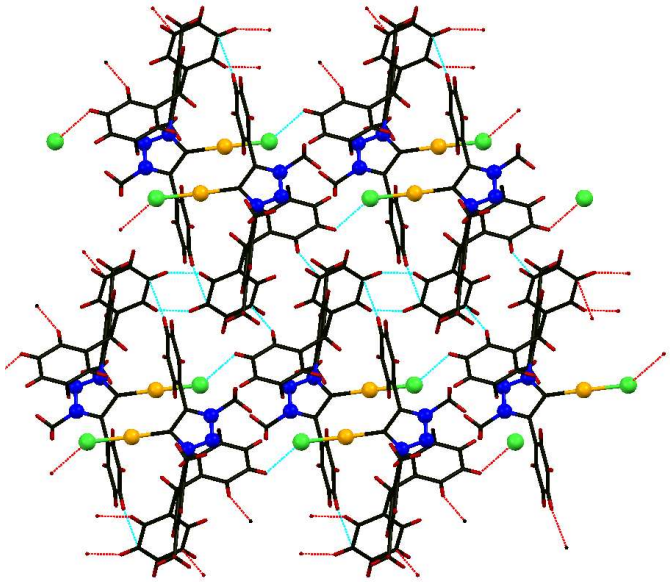

Fig. S17. Crystal packing of complex **1** shows intermolecular C- Cl···H interactions and (aryl)C-H···C (aryl) interactions. View along a axis.

DFT Calculations

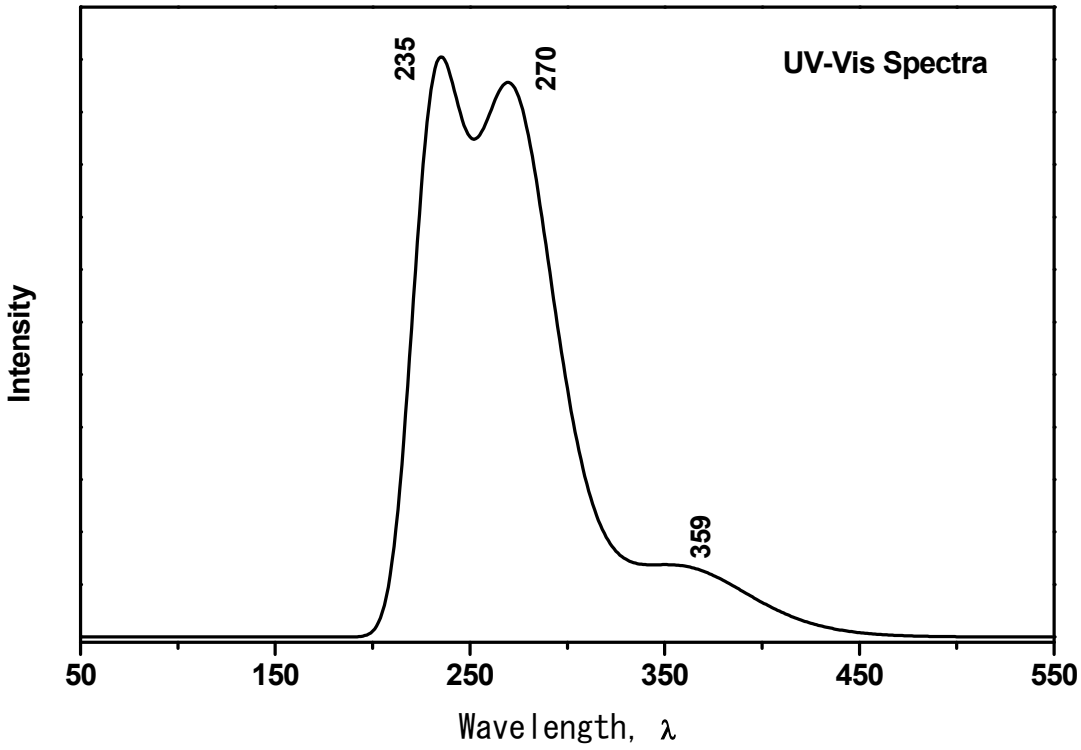

Fig. S18. The calculated UV-vis spectrum of **1**.

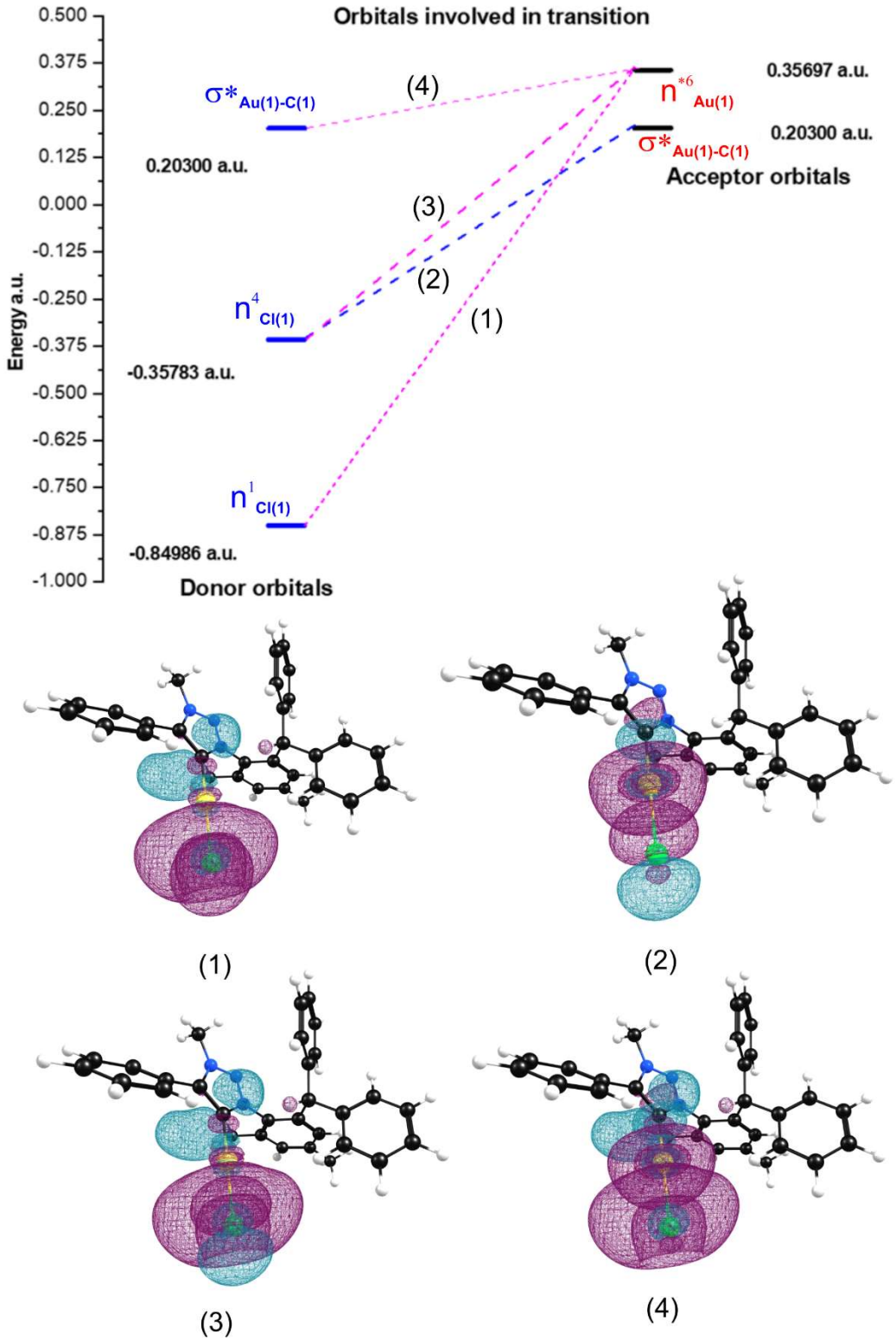

Fig. S19. The orbitals involved in the transition of **1**.

Table S1. Solid-state structural parameters of **1**.

Parameters	**1**
Empirical formula	$C_{30}H_{27}N_3AuCl_3$
Formula weight	661.99
Temperature (K)	298
Crystal system	triclinic
Space group	Pī
a/Å	10.0475(7)
b/Å	10.7852(5)
c/Å	13.3559(8)
α/°	103.912(4)
β/°	107.590(6)
γ/°	93.543(5)
Volume (Å^3)	1324.94(15)
Z	2
ρ_{calc}/mg mm^{-3}	1.6592
Absorption coefficient (μ/mm^{-1})	5.676
F(000)	644.9
Reflections collected	10483
R_{int}	0.0444
GOF on F^2	1.009
R_1 ($I>2\sigma(I)$)	0.0363
wR_2 ($I>2\sigma(I)$)	0.0675
R_1 values (all data)	0.0506
R_2 values (all data)	0.0795

Table S2. Fitting parameters of fluorescence decay of **1** in solution state ($1x10^{-5}$ M). (RAx = Relative amplitude of x^{th} component).

τ	τ1, ns	τ2,ns	A1	A2	χ^2	Decay	λ_{em}, 360 nm
2.40	1.26	4.99	33.77	3.75	1.07	2rd order	λ_{ex}, 280

Table S3. Fitting parameters of fluorescence decay of **1** in solution state ($1x10^{-6}$ M). (RAx = Relative amplitude of x^{th} component).

τ	τ1, ns	τ2,ns	A1	A2	χ^2	Decay	λ_{em}, 355 nm
3.73	1.36	5.27	26.39	10.45	1.05	2rd order	λ_{ex}, 280

Table S4. Fitting parameters of fluorescence decay of **1** in solution state ($1x10^{-7}$ M). (RAx = Relative amplitude of x^{th} component).

τ	τ1, ns	τ2,ns	A1	A2	χ^2	Decay	λ_{em}, 335 nm
3.14	0.86	4.13	12.39	6.27	1.02	2rd order	λ_{ex}, 280

Table S5. Fitting parameters of fluorescence decay of **1** (Crystal). (RAx = Relative amplitude of x^{th} component)

τ	τ_1	τ_2	τ_3	A1	A2	A3	χ2	Decay	Emission wavelength 435nm
94.619	0.1ms	21.14ms	98.74ms	1528.92	90.36	382.67	1.08	Third order	Excitation light 280nm

Tale S6. Excitation energies and oscillator strengths of **1**.

Orbitals involved in transition		Energy, eV	Wavelength, nm	Oscillator strength
HOMO-1 →LUMO HOMO →LUMO	0.36947 (27%) 0.59906 (72%)	3.4024	364.40	0.0213
HOMO-1 →LUMO+1 HOMO →LUMO+1	0.30833 (19%) 0.61396 (75%)	4.3214	286.91	0.0555
HOMO-9 →LUMO HOMO-8 →LUMO HOMO-7 →LUMO	0.46743 (44%) 0.43888 (38%) 0.26235 (13%)	4.4196	280.53	0.0128
HOMO-9 →LUMO HOMO-7 →LUMO HOMO-6 →LUMO	0.43368 (38%) -0.31564 (20%) -0.32496 (21%)	4.5749	271.01	0.1340
HOMO-3 →LUMO+1	0.65180 (85%)	4.6293	267.83	0.0158
HOMO-10 →LUMO HOMO →LUMO+3	0.59114 (70%) -0.26051 (13%)	4.6807	264.88	0.0164
HOMO-13 →LUMO HOMO →LUMO+3	0.42022 (35%) 0.46911 (44%)	4.7713	259.85	0.0152
HOMO-2 →LUMO+2 HOMO-1 →LUMO+4	-0.31754 (20%) 0.54896 (60%)	5.0731	244.40	0.0107
HOMO-2 →LUMO+2 HOMO-1 →LUMO+4	0.43413 (38%) 0.42655 (36%)	5.0925	243.46	0.0168
HOMO-3 →LUMO+2	0.66262 (88%)	5.2253	237.28	0.0180
HOMO-2 →LUMO+4 HOMO-2 →LUMO+5	0.45013 (40%) -0.24336 (12%)	5.3131	233.36	0.0259
HOMO-14 →LUMO HOMO →LUMO+6	-0.32531 (21%) 0.54424 (59%)	5.3228	232.93	0.0245
HOMO-14 →LUMO HOMO-6 →LUMO+1 HOMO-2 →LUMO+4 HOMO →LUMO+6	0.32767 (21%) 0.34834 (24%) -0.25192 (12%) 0.31378 (19%)	5.3449	231.97	0.0963
HOMO-14 →LUMO HOMO-6 →LUMO+1	0.43216 (37%) -0.33993 (23%)	5.3697	230.90	0.0105
HOMO-4 →LUMO+2 HOMO-2 →LUMO+3	0.37865 (28%) 0.26529 (14%)	5.4291	228.37	0.0365

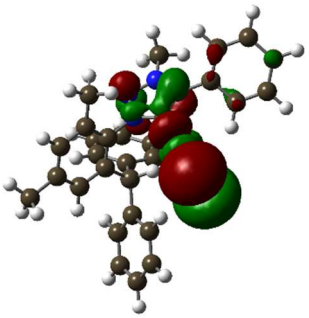

HOMO

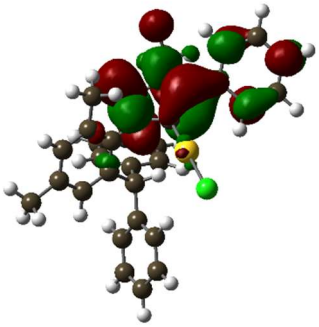

LUMO

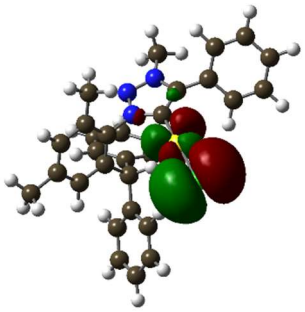

HOMO-1

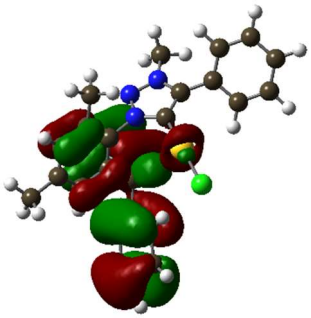

HOMO-2

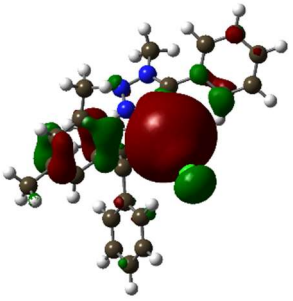

HOMO-3

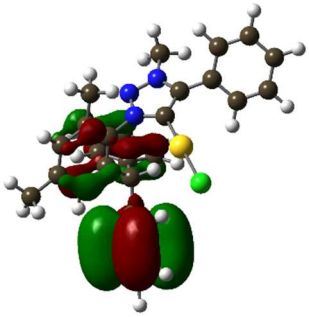

HOMO-4

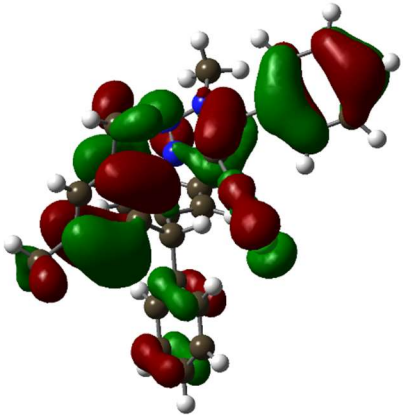

HOMO-6

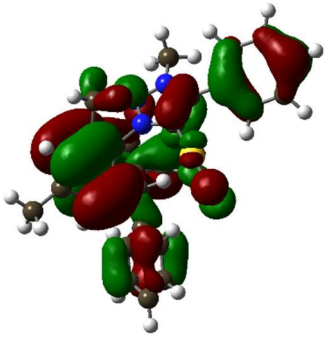

HOMO-7

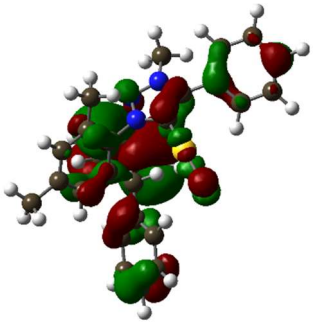

HOMO-8

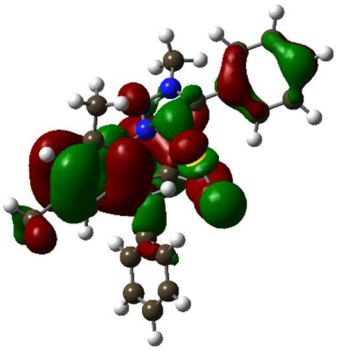

HOMO-9

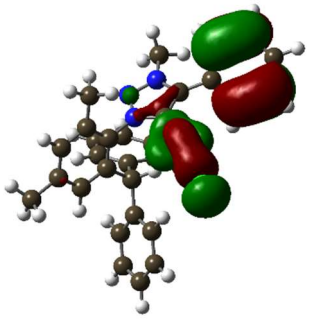

HOMO-10

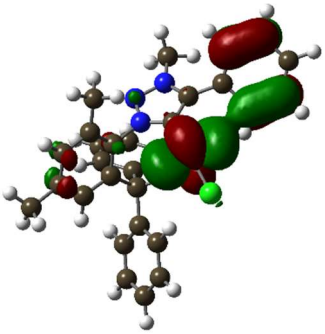

HOMO-13

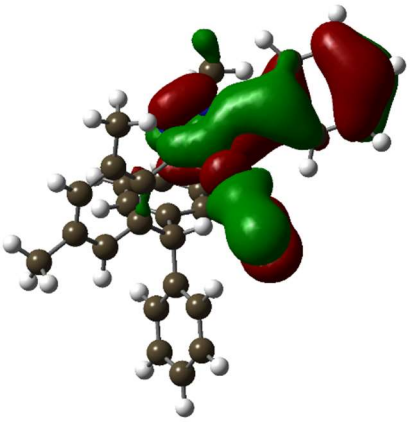

HOMO-14

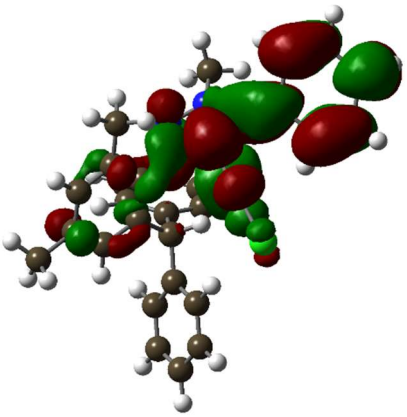

LUMO+1

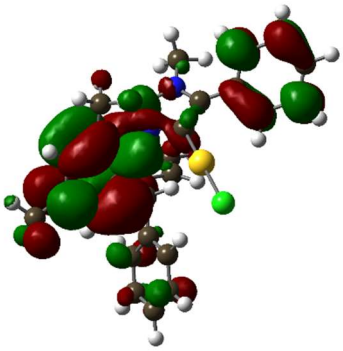

LUMO+2

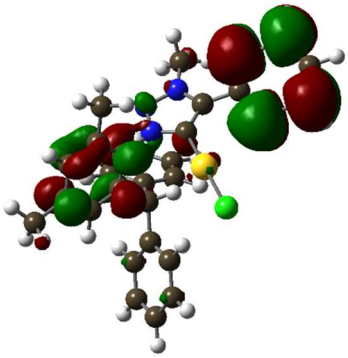

LUMO+3

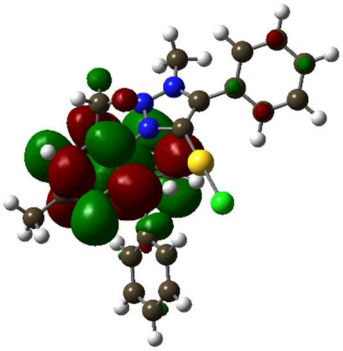

LUMO+4

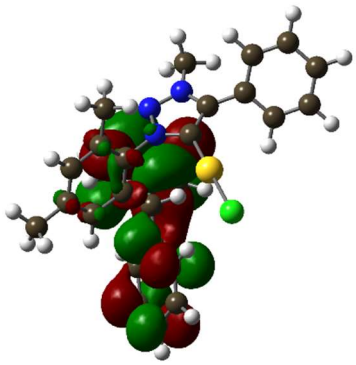

LUMO+5

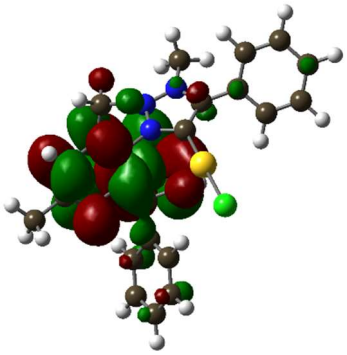

LUMO+6

Table S7. AIM Analysis (all in atomic units, a. u.)

Bond	ρ	$\nabla^2\rho$	λ_1	λ_2	λ_3	$\lvert\lambda_1\rvert/\lambda_3$
Au(1)-H56	0.0033	0.0100	-0.0020	-0.0015	+0.0135	0.1481
Au(1)-H22	0.0078	0.0259	-0.0042	-0.0029	+0.0330	0.1273
Au(1)-C(1)	0.1430	0.2412	-0.1717	-0.1657	+0.5785	0.2968

Table S8. NBO Analysis

Donor orbital (i)	Acceptor orbital (j)	ΔE kcal/mol	E_j-E_i a.u	F(i,j) a.u.
$n^{1}_{Cl(1)}$	$n^{*6}_{Au(1)}$	20.94	1.21	0.144

$n^4_{Cl(1)}$	$n^{*6}_{Au(1)}$	9.82	0.71	0.080
$n^4_{Cl(1)}$	$\sigma^*_{Au(1)-C(1)}$	92.34	0.56	0.206
$\sigma^*_{Au(1)-C(1)}$	$n^{*6}_{Au(1)}$	94.30	0.15	0.255

NBO	Occupancy	Energy	Hybridization	
$\sigma^*_{Au(1)-C(1)}$	0.28671	0.20300	(75.00%) 0.8660*Au(1)	s(78.24%)p 0.04(2.77%)d 0.24(18.90%) f 0.00(0.09%)
			(25.00%) -0.5000* C(1)	s(37.01%)p 1.70(62.99%)
$n^4_{Cl(1)}$	1.66523	-.35783	s(15.55%)p 5.43(84.45%)	
$n^1_{Cl(1)}$	1.98012	-0.84986	s(84.43%)p 0.18(15.57%)	
$n^{*6}_{Au(1)}$	0.07047	0.35697	s(3.48%)p26.62(92.59%)d 0.71(2.47%)f 0.42(1.46%)	

Table S9. DFT Cartesian coordinates of **1**.

Atom	X	Y	Z
N	1.7934904516	0.2122628597	4.9544533663
N	1.7691995472	1.4534179786	4.4055230535
N	1.3403451435	0.4158171684	6.2017956034
C	1.2532331579	1.6205653806	1.9998839621
C	3.0980911936	1.8307923374	0.3996866849
C	4.0121639871	1.8033184838	1.4612493701
H	5.0753947601	1.8807059678	1.2543613629
C	1.7274452101	1.738259783	0.6876775918
H	1.0103201446	1.7765954996	-0.1242021523
C	1.099116333	1.8161328877	8.9608044956
H	1.9346675677	1.1237395598	8.9632662285
C	-0.0953735385	-1.0388829472	2.1287738452
H	0.7337718258	-0.9309100022	1.4374117621
C	-0.693217648	0.1057826771	2.6799320574
C	-0.2482284519	1.5276374704	2.3132432165
H	-0.4095565241	2.1397295249	3.2092955921
C	2.2098576006	1.5955003424	3.0339304936
C	0.5402195329	2.2431179562	7.7388419246
C	3.5912873897	1.6890323711	2.7927526921
C	1.0413246662	1.744269109	6.4514811155
C	-0.4989466629	3.1948860916	7.7623123791
H	-0.9258030104	3.5417768419	6.8284643364
C	0.6187105651	2.3155919705	10.1741654864
H	1.0651312796	1.9842887077	11.1060104699
C	-0.4192128269	3.2542201279	10.186212841
H	-0.7874773148	3.6462298751	11.1284806076
C	-0.971511485	3.6949522398	8.977558692
H	-1.7684236929	4.4306814401	8.9785121041

C	-1.1198188655	2.1690776108	1.2223619769
C	-1.7562259187	-0.0621094638	3.5855459159
H	-2.2354652842	0.8155731531	4.0111236241
C	-2.2082891787	-1.338402768	3.9342402384
H	-3.0322276604	-1.4467884194	4.6332342534
C	-0.5476395643	-2.3184690523	2.4743602248
H	-0.0726112126	-3.1917979129	2.0378854075
C	3.5723867358	1.9948052836	-1.0266447151
H	4.5999851679	1.6386527632	-1.1515320673
H	2.933073931	1.4470927744	-1.7269411368
H	3.5517839365	3.0511695743	-1.325990988
C	4.5919545024	1.68300344	3.925018662
H	4.5308960439	0.7594415134	4.5124783386
H	5.6104640263	1.7708843303	3.5380570714
H	4.4193070168	2.5215698719	4.6106366758
C	-1.6035707369	-2.4736371453	3.3789498532
H	-1.9542944881	-3.4658088796	3.6456307554
C	1.1559079073	-0.7636573663	7.0546237055
H	0.9245308982	-1.6075087472	6.4056704799
H	2.0646756186	-0.9721792622	7.623462312
H	0.3292455212	-0.5759382634	7.7387210162
Au	1.1310131912	4.3920001517	4.7757170466
C	1.320774838	2.4497809951	5.2625329831
Cl	0.8614051826	6.6589367394	4.1984218975
C	-1.7701455378	1.4146796983	0.2331021994
H	-1.6863605816	0.3330864263	0.2379717676
C	-1.2619978891	3.5690178828	1.2096877565
H	-0.7649215865	4.1676956493	1.9687913194
C	-2.5413462571	2.0458395632	-0.751583804
H	-3.040312177	1.4475224495	-1.5079970857
C	-2.675099348	3.4381207481	-0.7575084643
H	-3.2763575447	3.926121237	-1.5182680019
C	-2.0328065111	4.198543784	0.2281245066
H	-2.132933376	5.2791699381	0.2372370933

References

1. Petronilho, H. Muller-Bunz and M. Albrecht, *Chem. Commun.,* 2012, **48,** 6499–6501; (b) T. Nakamura, T. Terashima, K. Ogata and S.-I. Fukuzawa, *Org. Lett.,* 2011, **134,** 620–623; (c) S. Hohloch, C.-Y. Su and B. Sarkar, *Eur. J. Inorg. Chem.,* 2011, **20,** 3067–3075.
2. (a) O. V. Dolomanov, L. J. Bourhis, R. J. Gildea, J. A. K. Howard and H. Puschmann, *J. Appl. Cryst.* **2009**, *42*, 339-341; (b) L. J. Bourhis, O. V. Dolomanov, R. J. Gildea, J. A. K. Howard, and H. Puschmann, *Acta Cryst.* **2015**, *A71*, 59-75.

3. Gaussian 16, Revision B.01, M. J. Frisch, G. W. Trucks, H. B. Schlegel, G. E. Scuseria, M. A. Robb, J. R. Cheeseman, G. Scalmani, V. Barone, G. A. Petersson, H. Nakatsuji, X. Li, M. Caricato, A. V. Marenich, J. Bloino, B. G. Janesko, R. Gomperts, B. Mennucci, H. P. Hratchian, J. V. Ortiz, A. F. Izmaylov, J. L. Sonnenberg, D. Williams-Young, F. Ding, F. Lipparini, F. Egidi, J. Goings, B. Peng, A. Petrone, T. Henderson, D. Ranasinghe, V. G. Zakrzewski, J. Gao, N. Rega, G. Zheng, W. Liang, M. Hada, M. Ehara, K. Toyota, R. Fukuda, J. Hasegawa, M. Ishida, T. Nakajima, Y. Honda, O. Kitao, H. Nakai, T. Vreven, K. Throssell, J. A. Montgomery, Jr., J. E. Peralta, F. Ogliaro, M. J. Bearpark, J. J. Heyd, E. N. Brothers, K. N. Kudin, V. N. Staroverov, T. A. Keith, R. Kobayashi, J. Normand, K. Raghavachari, A. P. Rendell, J. C. Burant, S. S. Iyengar, J. Tomasi, M. Cossi, J. M. Millam, M. Klene, C. Adamo, R. Cammi, J. W. Ochterski, R. L. Martin, K. Morokuma, O. Farkas, J. B. Foresman, D. J. Fox, Gaussian, Inc., Wallingford CT, **2016**.
4. GaussView, Version 6, R. Dennington, T. A. Keith, J. M. Millam, Semichem Inc., Shawnee Mission, KS, **2016**.
5. D. Andrae, U. Haeussermann, M. Dolg, H. Stoll, H. Preuss, *Theor. Chim. Acta* **1990**, 77, 123-141.
6. AIMAll (Version 19.10.12), T. A. Keith, TK Gristmill Software, Overland Park KS, USA, 2019.
7. R. F. W. Bader, *Atoms in Molecules: A Quantum Theory*; Oxford University Press: New York, 1990.